Physically Controlled Radical Polymerization of Vaporized Vinyl Monomers on Surfaces. Synthesis of Block Copolymers of Methyl Methacrylate and Styrene with a Conventional Free Radical Initiator

Mikio Yasutake, Shigehiro Hiki, Yoshito Andou, and Haruo Nishida*

HENKEL Research Center of Advanced Technology, Molecular Engineering Institute, Kinki University, 11-6 Kayanomori, Iizuka, Fukuoka 820-8555, Japan

Takeshi Endo*

Faculty of Engineering, Yamagata University, 4-3-6 Jyonan, Yonezawa, Yamagata 992-8510, Japan

Received December 30, 2002; Revised Manuscript Received May 13, 2003

ABSTRACT: Physically controlled radical polymerization of vinyl monomers with conventional free radical initiators was achieved in the presence of monomer vapors on solid substrate surfaces. The polymerization of methyl methacrylate (MMA) and styrene (St) by 2,2′-azobis(isobutyronitrile) (AIBN) on substrate surfaces resulted in the deposition of high molecular weight polymers, forming a rough surface morphology in such forms of aggregated particles. The proportional relationship between the number-average molecular weight and polymer yield was successfully obtained, and the consecutive copolymerization of MMA and St produced a block copolymer, poly(MMA-*b*-St). These results support the living nature of the free radical polymerization on surfaces in the presence of monomer vapors. The SEM observations of the deposits revealed that the polymerization proceeded with a continuous polymer deposition taking place at points where the active species were immobilized, reflecting a predesigned pattern on the substrate surface.

Introduction

Many living radical polymerization systems have been reported, including atom-transfer radical polymerization (ATRP),[1,2] nitroxide-mediated radical polymerization,[3] reversible addition−fragmentation chain transfer (RAFT),[4,5] iniferter,[6] and immortal polymerization.[7,8] These techniques realize the living nature of radical polymerization by controlling the equilibrium between active and dormant species and depressing the irreversible termination and chain transfer reactions.

Well-defined polymers and copolymers from conventional free radical polymerization have attracted great interest because the free radical polymerization is a robust and economical process and can use a wide range of monomers that have many applications. There are several reports of block copolymer preparation through macroradical approaches. Seymour and Stahl[9,10] reported a high level of block copolymer formation when the entrapped macroradicals of vinyl acetate and styrene (St) were produced in viscous poor solvents, e.g., silicone oils, and reacted with a second vinyl monomer. Sato et al.[11−13] and Kafetzopoulos et al.[14] prepared block copolymers by reacting occluded macroradicals of *N*-methyl methacrylamide with acrylates, St, and isoprene in benzene. Zhang et al.[15] reported the synthesis of poly(St-*b*-methyl methacrylate) via conventional free radical polymerization using benzoyl peroxide in ionic liquids by way of sequential monomer addition. These heterogeneous radical polymerizations entrapped propagating species in insoluble polymer particles and extended their lifetime. However, Louis et al.[16] reported that the entrapped macroradical model in a viscous solvent is doubtful in the dispersion polymerization of St and demonstrated that graft and statistical copolymers are formed in the process. Zhang et al.[15] also did not rule out the possibility of graft copolymer formation occurring in the consecutive copolymerization in ionic liquids.

This study examines a physically controlled process in gas-phase deposition polymerization (GDP) on surfaces with conventional free radical initiators. If a chain-end active species is placed at an interface between a gaseous monomer and a solid substrate surface, the lifetime of the species will be extended because termination and transfer reactions will be almost eliminated at the same time as propagation is continuing. In this situation, the propagation reaction may be dominant and continue to exhibit a living nature similar to the postulate of the entrapped macroradicals.

Many reports on gas-phase polymerizations have been published, for example, homogeneous gas-phase polymerization of styrene and vinyl acetate,[17−19] vapor deposition polymerization of vinyl monomers,[20−23] photoinduced vapor deposition polymerization,[24,25] and photoinduced graft polymerization in the gas phase.[26−29] El-Shall and Reiss[19] suggested that the homogeneous gas-phase polymerization by using a low concentration of initiating free radicals could eliminate termination processes. Recently, Bartlett et al.[30] reported a solventless deposition polymerization of fluorostyrene monomers with a peroxide initiator to prepare thin films. Hsieh and Zellers[31] also prepared thin films of silylated methacrylate monomers on substrates by UV photopolymerization in the vapor phase. Wang and Chang reported grafting of poly(γ-benzyl L-glutamate) on silicon native oxide surfaces by a surface-initiated vapor deposition polymerization and suggested the preparation of block co-polypeptides.[32] However, no report has clearly demonstrated the living nature of gas-phase deposition polymerization.

In this paper, the radical deposition polymerization and consecutive copolymerization of vapor-phase mono-

* Corresponding author: Tel/Fax +81-948-22-5706; e-mail hnishida@mol-eng.fuk.kindai.ac.jp.

10.1021/ma021795s CCC: $25.00
Published on Web 07/17/2003

mers on various surfaces were conducted with conventional free radical initiators to prepare block copolymers. A two-dimensional (2D) patterning was also examined using this GDP approach.

Experimental Section

Materials. Methyl methacrylate (MMA, >99.0%) and styrene (St, >99.5%) were obtained from Kishida Chemical Inc. and purified by distillation. 2,2′-Azobis(isobutyronitrile) (AIBN, >99%) was purchased from Otsuka Chemical Inc. and recrystallized from methanol. Benzoyl peroxide (BPO, 75%) was purchased from ACROS Organics and used as received. The polymerization inhibitor, 4-*tert*-butylprocatechol (>98%), was purchased from Tokyo Kasei Kogyo Co. Ltd. and used as received. Poly(methyl methacrylate) (PMMA, M_n 168 000 and M_w 335 000) and polystyrene (PSt, M_n 67 500 and M_w 321 000) were purchased from Aldrich (secondary polymer standard). Substrates, polyethylene (PE) films, and poly(tetrafluoroethylene) (PTFE) films {IR card for the infrared spectroscopy, 1.90 cm diameter (PE) and 1.38 cm diameter (PTFE), 3M}, glass slide, and aluminum pan (Al pan, 5 mm diameter) were used as purchased. All other reagents, such as cyclohexane (>98%), acetonitrile (>98%), acetone (>99%), chloroform (>99.0%), and methanol (>99%), were commercially obtained and purified by distillation.

Characterization Methods. ^{1}H NMR spectra were measured on 300 MHz JEOL AL-300 and 400 MHz Varian INOVA 400 VLX spectrometers. Chloroform-*d* was used as solvent. Chemical shifts were reported as δ values (ppm) relative to internal tetramethylsilane (TMS) in $CDCl_3$ unless otherwise noted. Fourier transform infrared (FTIR) spectroscopy was performed using a JASCO FT-IR 460 plus spectrometer. Reflection spectra of as-polymerized samples were measured on a Nicolet Thunderdome swap-top module with a germanium crystal by the single-reflection ATR method. Transmission spectra of purified samples were measured by coating the polymer solution on a KBr plate and evaporating the chloroform. Micro-IR measurements were performed on a Horiba FT-520W spectrometer. Transmission micro-IR spectra were taken from areas as small as 100 × 100 μm (aperture size).

Molecular weights of polymers were measured on a TOSOH HLC-8220 gel permeation chromatography (GPC) system with refractive index (RI) and ultraviolet (UV, $\lambda = 254$ nm) detectors under the following conditions: TSKgel Super HM-H linear column (linearity range, 10^3−8 × 10^6; molecular weight exclusion limit, 4 × 10^8), chloroform (HPLC grade) eluent at a flow rate of 0.6 mL min^{-1}, and column temperature of 40 °C. The calibration curves for GPC analysis were obtained using polystyrene standards with a low polydispersity (5.0 × 10^2, 1.05 × 10^3, 2.5 × 10^3, 5.87 × 10^3, 9.49 × 10^3, 1.71 × 10^4, 3.72 × 10^4, 9.89 × 10^4, 1.89 × 10^5, 3.97 × 10^5, 7.07 × 10^5, 1.11 × 10^6, TOSOH Corp.).

Scanning electron microscopy (SEM) for as-polymerized products and cast films was performed with a HITACHI S3000N, a JEOL JSM-5510LV, and a Philips XL30 scanning electron microscopes at an accelerating voltage of 15 kV with a backscattered electron (BSE) detector, a secondary electron (SE) detector, and an energy-dispersive X-ray spectrometer (EDX). Polymer films were prepared using a conventional solvent-casting technique from chloroform solutions of the polymers using glass Petri dishes as casting surfaces. The films were dried at 50 °C for 20 h in vacuo. The microscopes operated within a range of specimen chamber pressures from 15 to 75 Pa without an electron conductive layer of gold or carbon. The compositional and stereoscopic images were formed from BSE under the pressure conditions.

Differential scanning calorimetry (DSC) measurements were carried out under a nitrogen flow of 20 mL min^{-1} using a SEIKO Instruments Inc. EXSTAR6000-DSC6200 calibrated with indium. The film samples (2−3 mg) were encapsulated in aluminum pans and heated from 30 to 160 °C at a heating rate of 10 °C min^{-1}. The first, second, and third scans were recorded in all cases. The glass transition temperature (T_g) was taken as the midpoint of the heat capacity change in the third scan spectrum.

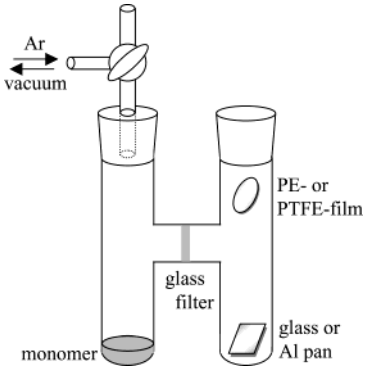

Figure 1. Gas-phase deposition polymerization apparatus; H-shaped glass tube reactor.

Homopolymerization. Homopolymerization was carried out in an H-shaped glass tube reactor with a vacuum cock and a glass filter separator (pore size 20−30 μm) at the bridge (Figure 1). The initiator (AIBN) solution (4.02 × 10^{-2} mol L^{-1}) was prepared with acetone. A 0.210 mL aliquot of the solution (AIBN 1.4 mg, 8.5 × 10^{-6} mol) was spread on an Al pan surface (5 mm diameter). The substrate was dried for 2 h at ambient temperature in a desiccator at atmospheric pressure and then for a further 15 min under reduced pressure (13 Pa) before being set in the bottom of one of the legs of the H-shaped glass tube reactor. MMA (0.5 mL) and 4-*tert*-butylpyrocatechol (20 mg, 1.2 × 10^{-4} mol) were introduced into the bottom of the other leg. The reactor was degassed by three freeze−pump−thaw cycles and then sealed under a saturated atmosphere of MMA. Polymerization was carried out at 55 °C for 5.5 h under a saturated vapor pressure of 1.86 × 10^4 Pa in an oven. After the reaction, the sample, on which polymer was formed, was dried to remove the adsorbed MMA in vacuo and weighed to obtain a polymer of 50.0 mg (sample 1-2 in Table 1). The polymer was analyzed intact by FTIR, ^{1}H NMR, and GPC and then dissolved in chloroform, followed by precipitation with methanol. The purified polymer was also analyzed by ^{1}H NMR and GPC. The analytical results were as follows: FT-IR (cm^{-1}): 1733 ($\nu_{C=O,ester}$). ^{1}H NMR (δ, ppm): 3.65 (−OC***H***$_3$, 3H), 2.08−1.31 (−C***H***$_2$−, 2H), 1.23−0.75 (−C***H***$_3$, 3H). GPC (RI, $CHCl_3$): M_n 265 000 and M_w 1 350 000. These results agreed with the characteristic data of commercially obtained PMMA. The polymerizations of MMA and St were carried out under different conditions as listed in Table 1 to give the corresponding homopolymers.

Time-course tests were conducted on the Al pans coated with initiator in the H-shaped glass tube reactor and repeating the following cycle after being charged with monomer, that is, three times of freeze−pump−thaw cycle, degassing, GDP at prescribed temperature, cooling to ambient temperature, and sampling some Al pans under Ar flow.

Copolymerization. Copolymerization of MMA and St in the gas phase was carried out both consecutively and simultaneously. In the case of consecutive copolymerization, the first stage was conducted in a similar way to the homopolymerization. The initiator solution (AIBN, 4.02 × 10^{-2} mol L^{-1}) was prepared with acetone. A 0.485 mL aliquot of the solution (AIBN 3.2 mg, 1.9 × 10^{-5} mol) was spread on a glass plate surface (1.1 cm^2). The substrate was dried for 2 h at ambient temperature in a desiccator and for 15 min under reduced pressure (13 Pa) and then set in the bottom of one of the legs of the H-shaped glass tube reactor. MMA (0.5 mL) and 4-*tert*-butylpyrocatechol (20 mg, 1.2 × 10^{-4} mol) were added in the bottom of the other leg. The reactor was degassed by three freeze−pump−thaw cycles and then sealed in a saturated atmosphere of MMA. Polymerization was carried out at 60 °C for 2 h under a saturated vapor pressure of 2.34 × 10^4 Pa in an oven. After the first stage, the reactor was cooled to room temperature, and the remaining MMA was removed in vacuo. Next, the second monomer, St, (0.5 mL), was introduced into

Table 1. Deposition Polymerization of Vaporized MMA and St on Substrate Surfaces

	monomer[a]		initiator				polymerization			GPC_{RI}	
sample		($\times 10^4$ Pa)[b]		(mg)	(μmol cm^{-2})	substrate	(°C)	(h)	yield (mg)	M_n	PDI
1-1	MMA	1.49	AIBN	2.5	10.5	PE film	50	17.5	nd[c]	741 000	2.1
1-2	MMA	1.86	AIBN	1.4	43.4	Al pan	55	5.5	50.0	265 000	5.1
1-3	MMA	1.86	AIBN	1.0	31.0	Al pan	55	5	33.6	224 000	6.0
1-4	MMA	1.86	AIBN	0.7	21.7	Al pan	55	5	19.5	185 000	6.9
1-5	MMA	1.49	BPO	0.45	2.1	Al pan	50	4	10.2	216 000	4.8
1-6	St	0.85	AIBN	0.5	15.5	Al pan	60	5	1.0	10 400	1.8
1-7	St	0.85	AIBN	26.4	321.6[d]	PMMA[e]	60	2.5	28.5	165 000[f]	2.0

[a] 0.5 mL. [b] Saturated vapor pressure. [c] Not determined. [d] In μmol. [e] M_n 168 000, PDI 1.99, 45.90 mg. [f] PMMA−PSt.

Table 2. Consecutive and Simultaneous Deposition Copolymerization of Vaporized MMA and St on Substrate Surfaces

	monomer[a] ($\times 10^4$ Pa)		AIBN			polymerization (h/°C)		yield	unit ratio[b]	GPC_{RI}[c]			
sample	1st-MMA	2nd-St	(mg)	(μmol cm^{-2})	substrate	1st-MMA	2nd-St	(mg)	[MMA]:[St]	Mn_{RI}	PDI_{RI}	Mn_{UV}	PDI_{UV}
Consecutive													
2-1c	1.49	0.58	2.9	19.8	glass	12/50	12/50	8.2	0.43:0.57	516 000	2.36	486 000	2.35
2-2c	2.34	0.85	3.2	21.7	glass	2/60	4/60	97.3	0.29:0.71	126 000	5.51	146 000	4.75
2-3c	2.34	0.85	5.0	33.8	glass	2/60	5/60	168.8	0.34:0.66	211 000	4.39	196 000	4.49
2-4c	1.49	0.58	3.1	13.0	PTFE film	12/50	11/50	87.8	0.86:0.14	486 000	3.47	849 000	2.13
Simultaneous													
2-5s	2.06		2.9	12.2	PTFE film	8/60		33.9	0.54:0.46	40 500	5.51	35 800	6.36
2-6s	2.06		2.2	14.9	glass	8/60		15.3	0.52:0.48	42 400	4.78	34 500	5.04

[a] Saturated vapor pressure. [b] Calculated from peak intensities of a singlet at 3.65 ppm (−COOC$\boldsymbol{H}_3$ in MMA unit) and signals at 6.38−7.16 ppm (aromatic protons in St unit) in ^{1}H NMR spectra. [c] As-polymerized sample.

Table 3. Composition of GDP Samples Fractionated by Selective Solvent Extraction

	cyclohexane extracted[a]					acetonitrile extracted[b]					chloroform extracted[c]						
		(unit %)[e]					(unit %)[e]					(unit %)[e]					
sample	(wt %)	St	MMA	M_n[f]	PDI[f]	(wt %)	St	MMA	M_n	PDI	(wt %)	St	MMA	M_n	PDI	loss[d] (wt %)	insoluble residue (wt %)
2-2c	7.9	100	0	118 000	3.87	10.9	0	100	143 000	3.79	80.9	66.7	33.3	380 000	2.26	0.3	0
1-7	37.2	100	0	298 000	1.53	62.8	7.0	93.0	154 000	1.78	0	−	−	−	−	0	0

[a,b] Extraction for 24 h at 80 °C. [c] Extraction at rt. [d] Loss during the extraction process. [e] Calculated from peak intensities of a singlet at 3.65 ppm (−COOC$\boldsymbol{H}_3$ in MMA unit) and signals at 6.38−7.16 ppm (aromatic protons in St unit) in ^{1}H NMR spectra. [f] Calculated from GPC profile monitored with RI detector on the basis of PSt standards.

the bottom with a syringe through the glass cock of the reactor under Ar gas flow. The reactor was degassed again by three freeze−pump−thaw cycles and then sealed under a saturated atmosphere of St. The second stage was also carried out at 60 °C for 4 h under a saturated vapor pressure of 0.85×10^4 Pa without any additional initiator. After the reaction, the polymer formed on the glass plate was dried in vacuo and weighed to obtain a polymer of 97.3 mg (sample 2-2c in Table 2). The polymer was characterized by a similar way to the homopolymerization. The analytical results were as follows: FT-IR (cm^{-1}): 1733 ($\nu_{C=O,ester}$). ^{1}H NMR (δ, ppm): 3. 65 (−OC$\boldsymbol{H}_3$), 2.08−1.31 (−C$\boldsymbol{H}_2$− and ⟩C$\boldsymbol{H}$−), 1.23−0.75 (−C$\boldsymbol{H}_3$), 6.3−7.2 (aromatic protons), unit ratio [MMA]:[St] = 0.29:0.71. GPC (RI and UV, $CHCl_3$): $M_{n,RI}$ 126 000, $M_{w,RI}$ 694 000, $M_{n,UV}$ 146 000, and $M_{w,UV}$ 695 000. The copolymerizations of MMA and St were carried out under different conditions as listed in Table 2 to give the corresponding copolymers.

In the case of the simultaneous copolymerization, comonomers were added together for a one-step process (see Supporting Information). The reaction and product characterizations were run using the same process as for the consecutive copolymerization (Table 2).

The crude copolymer sample 2-2c (56.70 mg) was extracted to remove each homopolymer at 80 °C for 24 h using selective solvents, i.e., cyclohexane for PSt and acetonitrile for PMMA.[15,16,33,34] After the selective extraction, the residue was dissolved in $CHCl_3$ at room temperature. The fractions (7.9, 10.9, and 80.9 wt %) were characterized with ^{1}H NMR (see Supporting Information), FTIR, and GPC (Table 3).

Graft Reaction. The graft reaction of St on PMMA was examined in a similar way to the homopolymerization of St except that PMMA substrate was used (M_n 168 000, M_w 335 000). The PMMA powder (45.90 mg) and the initiator solution (4.02×10^{-2} mol L^{-1} in acetone, 4 mL; AIBN, 26.37 mg) were mixed in one of the bottom legs of the H-shaped glass tube reactor, the PMMA was dissolved, and then acetone was removed initially at ambient temperature for 12 h and subsequently for 15 min in vacuo, producing an AIBN-impregnated PMMA thin film substrate on the reactor bottom surface. After the preparation of the initiator-impregnated PMMA substrate, GDP of St (0.5 mL) on the substrate was carried out at 60 °C for 2.5 h under a saturated vapor pressure of St (0.85×10^4 Pa). After the reaction, the PMMA substrate was dried to remove the adsorbed St in vacuo and weighed to obtain an additional polymer of 28.5 mg (sample 1-7 in Table 1). Sample 1-7 was analyzed by ^{1}H NMR and GPC (Table 1). The result of ^{1}H NMR analysis was as follows: ^{1}H NMR (δ, ppm): 3. 65 (−OC$\boldsymbol{H}_3$), 2.08−1.18 (−C$\boldsymbol{H}_2$− and ⟩C$\boldsymbol{H}$−), 1.05−0.75 (−C$\boldsymbol{H}_3$), 6.3−7.2 (aromatic protons), unit ratio [MMA]:[St] = 0.63:0.37.

The crude sample 1-7 was extracted to remove each homopolymer using the selective solvents in the same manner as the sample 2-2c. The fractions (37.2, 62.8, and 0 wt %, respectively) were characterized with ^{1}H NMR (see Supporting Information), FTIR, and GPC (Table 3).

Results and Discussion

Homopolymerization. The GDP of MMA and St was carried out on polyethylene film (IR card) and aluminum pan (Al pan) surfaces coated with AIBN and BPO under a saturated atmosphere of each monomer (Table 1). The formed PMMA (sample 1-1) was detected intact by FTIR (Figure 2). The polymerizations by AIBN proceeded smoothly at 55−60 °C on the surfaces (samples 1-2−1-4), and no polymer appeared on the substrate

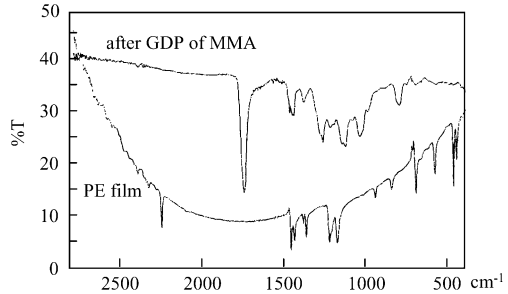

Figure 2. IR spectrum of PMMA deposited at 50 °C for 21 h on PE film coated by AIBN in the gas phase.

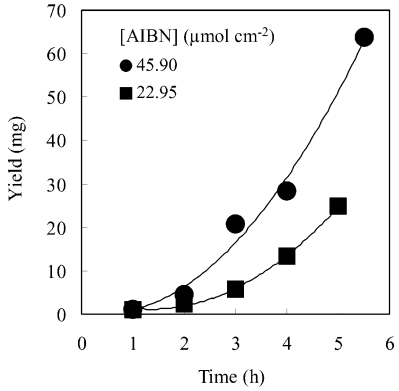

Figure 3. Changes in polymer yield on GDP of MMA with different concentrations of AIBN at 55 °C. Substrate, Al pan; [AIBN] = 45.90 ± 5.34 (sample 1-2), and 22.95 ± 1.52 μmol cm^{-2} (sample 1-4).

surfaces without the initiator. The polymerization by BPO also proceeded smoothly on the Al pan surface at 50 °C (sample 1-5); however, on other substrates such as the IR card and glass plate the GDP by BPO required further conditions such as a higher temperature or a longer reaction time to produce a polymer. The homopolymers PMMA and PSt obtained by the GDP were completely soluble in conventional solvents for corresponding polymers prepared by a common liquid process. Based on GPC analysis, the polymers were of a high molecular weight (10^4−10^6 Da in M_n). FTIR and ^{1}H NMR spectra of the PMMA showed a sharp peak at 1730 cm^{-1} and a sharp singlet at 3.65 ppm assigned to $\nu_{C=O}$ and −COOC***H*****$_3$**, respectively. Similarly, the FTIR and ^{1}H NMR spectra of PSt prepared by the GDP had characteristic signals at 1750−2000 cm^{-1} and 6.38−7.16 ppm assigned to $\delta_{\text{aromatic C−H}}$ and aromatic protons, respectively.

Figure 3 shows the changes in polymer yield on the GDP of MMA with different surface concentrations of AIBN. The GDP accelerated gradually as a function of time and increasing initiator concentration. This may be due to changes in the condition of the surface and surroundings of the active species. It can be assumed that the GDP proceeds via adsorption and diffusion processes of monomer molecules on a substrate surface. The adsorption and diffusion behavior of monomer molecules will depend on the surface area and polymer mass on the substrate surface. In particular, aggregated microparticles, microapertures, and micropores, which were the typical surface morphology after GDP (see Figure 10 and Supporting Information), will affect the adsorption and diffusion behavior of the monomer and the propagation behavior of the active species. The rough surface increases the absorption of the monomer, and the internal condition of microapertures and pores

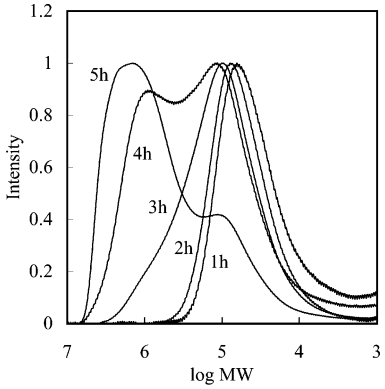

Figure 4. Change in GPC profile on GDP of MMA with AIBN at 55 °C (sample 1-4). Substrate, Al pan; [AIBN] = 22.95 ± 1.52 μmol cm^{-2}.

may approximate to a bulk. When a growing end radical is isolated in such a microaperture or pore, the propagation will be accelerated. Thus, the GDP might be accelerated with an increase in the surface area and/or polymer mass.

Changes in the GPC profile of PMMA formed at 55 °C are illustrated in Figure 4. The profiles shifted to higher molecular weights with time, maintaining a unimodal profile up to 3 h, and then gradually changing into a bimodal or multimodal profile. Plots of M_n vs PMMA yield were relatively linear up to 250 000 in M_n (Figure 5a). The slope of the plot increased as the initiator concentration diminished. However, each plot of M_n vs PMMA yield per initiator concentration on the substrate surface converged to one line (Figure 5b). These results suggest that the growing chain ends continued to propagate with a long lifetime, and after an initial period the subsequent initiation process was reduced. Considering the 10 h half-life temperature of AIBN is 65 °C, a considerable amount of AIBN must have continued to generate radical species during the GDP at 55 °C. However, the GPC profiles do not show newly occurring polymer chains, which should appear in the lower molecular weight region. From SEM observation of the as-polymerized surface, the deposited polymer molecules accumulated on the substrate surface (see Supporting Information). Thus, the remaining AIBN molecules on the surface were apparently buried under the accumulated deposits.

The GPC profile of PSt prepared by the GDP also shifted monotonically to a higher molecular weight region up to 10 400 in M_n, maintaining a relatively unimodal profile (PDI = 1.8−2.5) (sample 1-6 in Table 1). Similarly, a linear relationship between M_n and PSt yield was obtained (see Supporting Information).

The time-course test results of the GDP with MMA and St indicated that the growing chain ends had a long lifetime on the surfaces.

Copolymerization. MMA and St were copolymerized both consecutively and simultaneously under the conditions listed in Table 2. In the consecutive copolymerizations, after the first-stage reaction the remaining MMA was thoroughly distilled away in vacuo and then followed by the introduction of St to start the second-stage reaction. The simultaneous copolymerizations were carried out with mixed gaseous monomers. Both copolymerizations proceeded smoothly to produce copolymers with both MMA and St units. The compositions were calculated from the peak intensities of the singlet at 3.65 ppm (−COOC***H*****$_3$** in MMA unit) and the

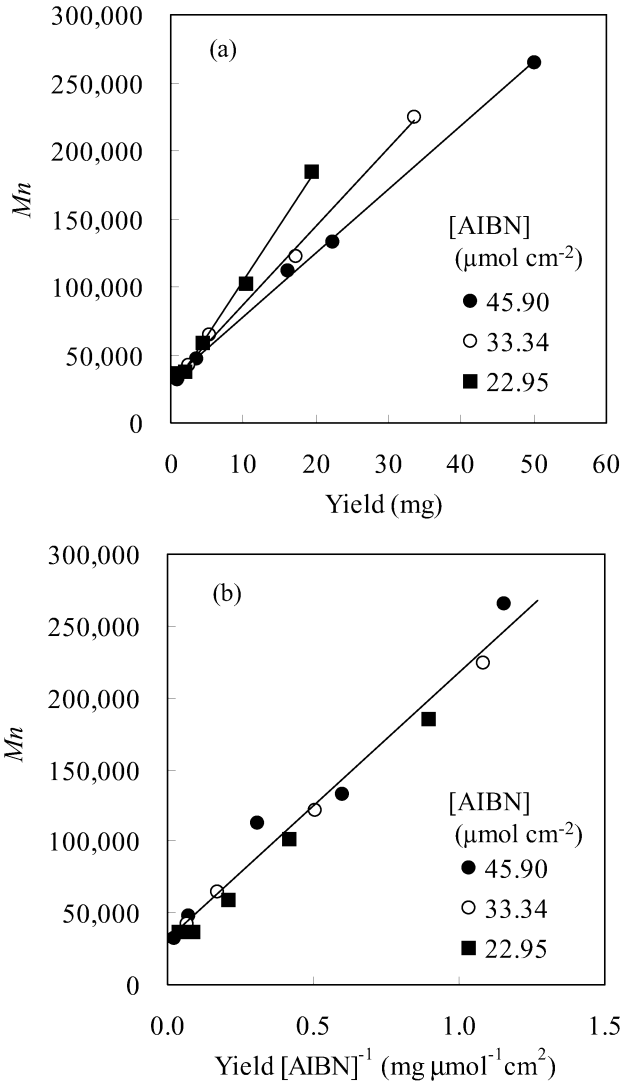

Figure 5. Plots of M_n vs polymer yield on GDP of MMA with different concentrations of AIBN at 55 °C. Substrate, Al pan; [AIBN] = 45.90 ± 5.34 (●, sample 1-2), 33.34 ± 2.57 (○, sample 1-3), and 22.95 ± 1.52 μmol cm^{-2} (■, sample 1-4).

signals at 6.38−7.16 ppm (aromatic protons in St unit) in ^{1}H NMR spectra and from the fraction intensities of GPC profiles monitored by RI and UV detectors. Copolymers in the composition range of [MMA]:[St] = 0.29:0.71−0.86:0.14 unit ratio were prepared under different copolymerization conditions (Table 2).

In Figure 6, a typical ^{1}H NMR spectrum of the consecutive copolymerization sample 2-2c ([MMA]:[St] = 0.29:0.71 unit ratio) is compared with that of a simultaneous copolymerization sample 2-5s ([MMA]:[St] = 0.54:0.46 unit ratio). A sharp singlet at 3.65 ppm assigned to −COOC$\boldsymbol{H}_3$ is present in the spectrum of sample 2-2c, while the spectrum of sample 2-5s has split peaks (*X*, *Y*, and *Z* in Figure 6) due to the MMA unit in the random copolymer.[15,33,35,36] The peak profile in the range of δ 6.3−7.2 ppm of the sample 2-2c also indicates the characteristic profile of aromatic ring protons in a continuous St unit sequence,[15,33,37] in contrast to the peak profile of the sample 2-5s in the range of 6.7−7.3 ppm, which indicates that the aromatic ring protons are in a random sequence of MMA and St units. Therefore, sample 2-2c is most likely a block or graft copolymer and/or a blend of each homopolymer.

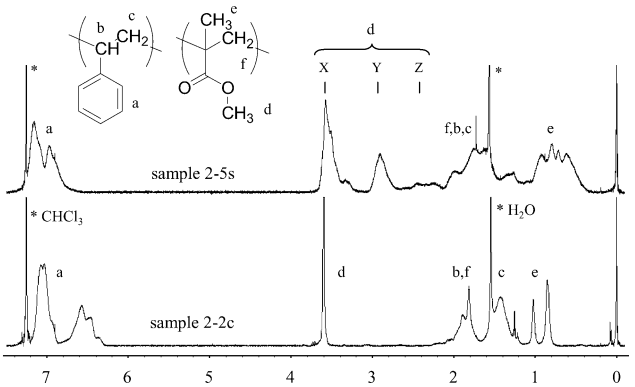

Figure 6. ^{1}H NMR spectra of the consecutive copolymerization product, sample 2-2c, and the simultaneous copolymerization product, sample 2-5s. Peaks, X, Y, and Z, are −OC$\boldsymbol{H}_3$ resonances of the MMA−St copolymer and have been assigned, by considering the nature and the configuration of neighboring units in relation to the central methyl methacrylate unit in the triad, as follows: *X*: P[MMM] + 2(1 − σ)P[MMS] + (1 − σ)^2P[SMS]; *Y*: 2σP[MMS] + 2σ(1 − σ)P[SMS]; and *Z*: σ^2P[SMS], where M and S represent MMA and St units, respectively, P[MMS], P[MMS], P[SMM], and P[SMS] are mole fractions of the triads, and parameter σ is a probability of alternating M and S units taking the same configurations.[37]

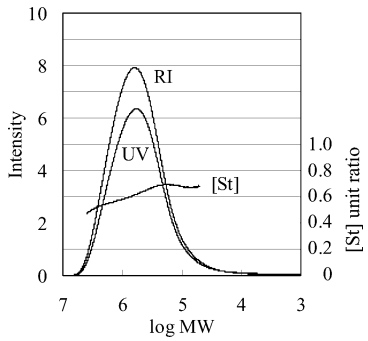

Figure 7. GPC profiles monitored by RI and UV detectors and [St] unit ratio of the fractionated copolymer sample 2-2c.

To examine the possibility of graft copolymer production in the GDP process, the GDP of St was conducted on a PMMA substrate impregnated with AIBN to prepare a complex sample 1-7 with a unit ratio: [MMA]:[St] = 0.63:0.37 (Table 1). To determine the copolymer structure, the selective solvent fractionation method[15,16,33,34] was applied to the GDP samples. The crude products were extracted to remove each homopolymer at 80 °C for 24 h using the selective solvents, cyclohexane and acetonitrile for PSt and PMMA, respectively. If a polymer is a blend of each homopolymer, the polymer should be completely fractionated by the method (see Supporting Information). Results of the selective solvent fractionation of samples 2-2c and 1-7 are listed in Table 3. The consecutive copolymerization sample 2-2c included a high level (80.9 wt %) of copolymer component and small amounts of PMMA (10.9 wt %) and PSt (7.9 wt %) homopolymers. Sample 1-7 polymerized on the PMMA substrate was mostly composed of a blend of homopolymers and may include a small amount of grafted component. Both samples did not include any cross-linked insoluble residue. Therefore, these results strongly suggest that the consecutive GDP sample is rich in a block structure, but neither a graft copolymer nor a simple blend.

Figure 7 shows the GPC profiles of the fractionated copolymer sample 2-2c monitored with RI and UV detectors. Because the absorption of UV (λ = 254 nm)

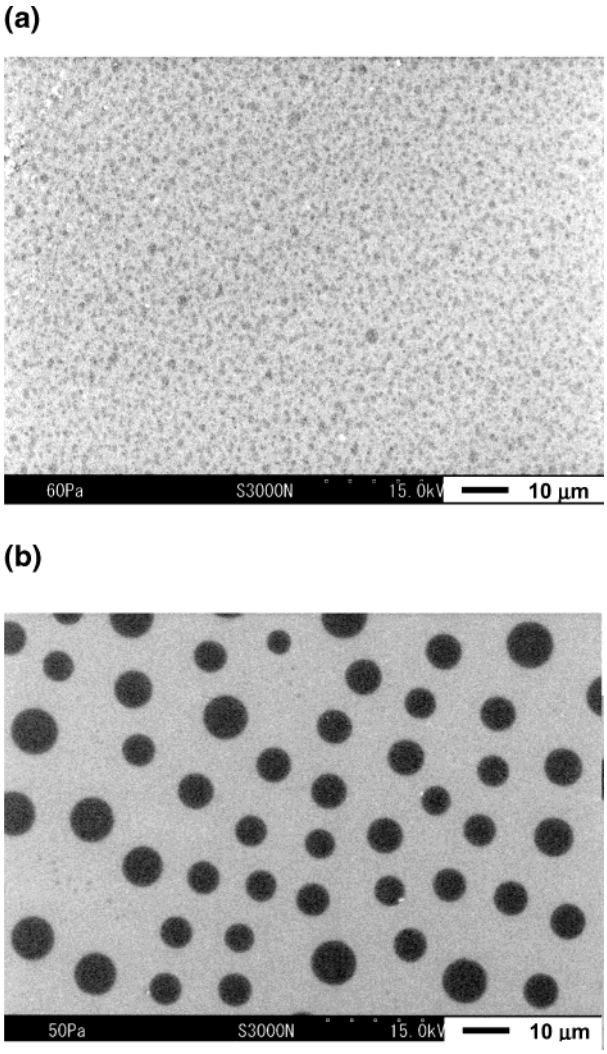

Figure 8. Compositional SEM images of consecutive GDP sample 2-2c (a) (×1000) and a PMMA/PSt blend (b) (×1000) films.

by the MMA unit can be considered to be negligible compared to that of the St unit, the GPC profile monitored by UV detector can be regarded as the distribution of St unit. Both RI and UV profiles were of a similar shape and of similar numerical values in average molecular weights despite relatively high PDI as 2.26.[38] The St unit ratio of each fraction in the GPC profile was nearly constant in the range 0.5−0.7 over the whole peak profile. Considering the accuracy of the composition value, as calculated based on the RI and UV intensities of each GPC fraction, the unit ratio range is relatively close to the value [St] = 0.667 calculated from the peak intensities of the ^{1}H NMR spectrum. This result indicates that the block structure of the sample 2-2c is statistically homogeneous over almost all fractions in the GPC profile. Other samples, 2-1c and 2-3c in Table 2, prepared by the consecutive copolymerization also exhibited similar GPC profiles monitored with RI and UV detectors (see Supporting Information).

The phase-separation behavior of copolymers can confirm a block structure of P(MMA-*co*-St).[39,40] Compositional SEM images of the cast films from the as-polymerized samples 2-2c (M_n 126 000, PDI 5.51) and PMMA/PSt blend are shown in Figure 8, in which the SEM images were formed from the backscattered electrons (BSE). The blend was composed of the same unit ratio [MMA]:[St] = 0.29:0.71 of PMMA (M_n 168 000, PDI 1.99) and PSt (M_n 67 500, PDI 3.42) as that of sample 2-2c. From the energy-dispersive X-ray spectrometer (EDX) analysis, bright and dark areas in the images were revealed as MMA unit-rich and St unit-rich regions, respectively (Figure 8a). The blend film clearly shows a macroscopic phase separation in the diameter range of 5−10 μm (Figure 8b), while the SEM image of sample 2-2c film showed disordered microdomains of less than 1 μm in diameter with poor contrast (Figure 8a). These images indicate that the sample 2-2c is not a simple blend. The disordered microdomains and poor contrast would be due to the high PDI of sample 2-2c, in which short segments may be brought into another kind of domain.

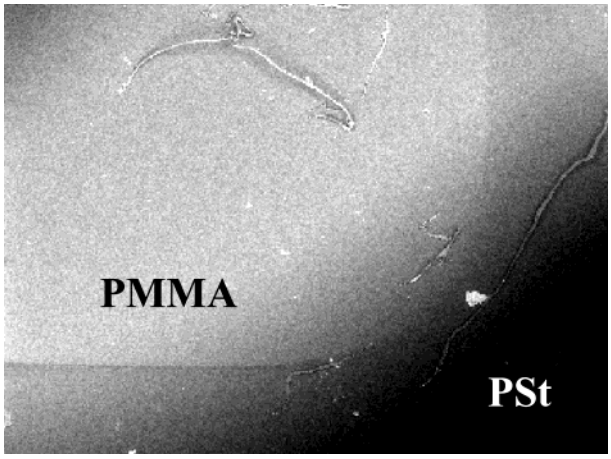

Figure 9. Compositional SEM image (×35) of as-polymerized sample 2-2c on a glass plate.

The thermal property of a consecutive copolymerization sample 2-4c ([MMA]:[St] = 0.86:0.14 unit ratio) was characterized by DSC analysis and compared to the random copolymer sample 2-5s and a PMMA/PSt blend ([MMA]:[St] = 0.86:0.14 unit ratio). The DSC thermogram of the sample 2-4c film showed two distinct glass transitions (T_g) at 121.8 and 100.0 °C, which correspond to the PMMA and PSt domains, respectively. The thermograms of the random copolymer and blend films showed the T_g at 92.1 °C (random copolymer) and 122.6/99.0 °C (blend). The T_g values of the sample 2-4c film are obviously close to those of the blend. These results suggest that the PMMA and PSt domains in sample 2-4c is phase-separated enough to exhibit the same T_g values as those of the blend. A similar phase-separation result was observed in the DSC thermogram of sample 2-2c.

SEM Observation of Deposition. A cross-sectional SEM image of the as-polymerized sample 2-2c with the BSE detector is shown in Figure 9. The bright and dark areas indicate the PMMA-rich and PSt-rich regions, respectively. A boundary line was clearly observed according to the consecutive process of the GDP. This SEM image demonstrates that the GDP proceeded with an accumulation of polymer layers on the deposited surface, not by swelling up in the polymer matrix.

To confirm a potentiality of the GDP for a two-dimensional (2D) patterning on substrate surfaces, MMA was polymerized on a polyethylene film, on which prepatterned lozenge basins (size: 80 × 150 μm; depth: 5−10 μm) were arranged at intervals of 500 μm (Figure 10b). The initiator, AIBN, was solvent-cast on the PE film surface. From the micro-IR observation, AIBN was relatively concentrated on the surfaces of the

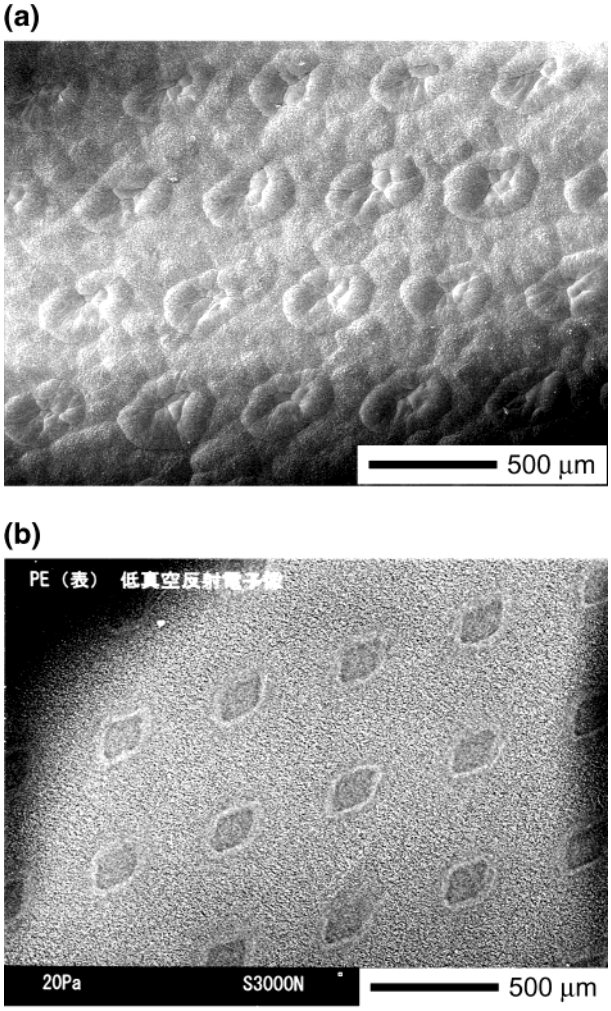

Figure 10. 2D-pattern (a) formed by GDP of MMA on the prepatterned PE-film surface (b) (sample 1-1).

basins more than matrix surface. The GDP of MMA was carried out at 50 °C for 17.5 h to produce a PMMA deposition covering the surface (sample 1-1 in Table 1). The deposited polymer was of a high molecular weight PMMA (M_n 741 000, M_w 1 560 000) from GPC analysis. The SEM image of the as-polymerized sample 1-1 surface exhibited aggregates of microparticles (1−2 μm in diameter) covering the substrate surface (Figure 10a and see Supporting Information). In particular, specific petallike structures that had risen up on the surface were observed. The structures were arranged at intervals of 500 μm to show the 2D pattern, which obviously reflected the prepatterned basin arrangement. This result also means that the deposition was piled up high at each point on the surface, where the active species were immobilized.

Conclusions

The deposition polymerization in monomer vapor of MMA and St by conventional free radical initiators resulted in the formation of high molecular weight polymers on some substrate surfaces. The proportional relation between the number-average molecular weight and polymer yield was obtained. The consecutive copolymerization led to the formation of block copolymers. These results support the living nature of the GDP process, in which active species at growing chain ends are immobilized on the deposition surface. That is, the GDP is the physically controlled process. The SEM observations of the deposits revealed that the GDP proceeded with continuous polymer deposition at points where the active species were immobilized, reflecting a predesigned pattern on the substrate surface.

Acknowledgment. The authors gratefully acknowledge the financial support by Henkel KGaA.

Supporting Information Available: Relationship between M_n and PSt yield on GDP of St, ^{1}H NMR spectra of fractionated components of samples (2-2c and 1-7) and a simple blend of PMMA and PSt by the selective solvent fractionation method, GPC profiles of samples 2-1c, 2-3c, and 2-5s monitored by both RI and UV detectors, and SEM images of the deposition surface of sample 1-1. This material is available free of charge via the Internet at http://pubs.acs.org.

References and Notes

(1) Matyjaszewski, K.; Xia, J. *Chem. Rev.* **2001**, *101*, 2921−2990.
(2) Kamigaito, M.; Ando, T.; Sawamoto, M. *Chem. Rev.* **2001**, *101*, 3689−3745.
(3) Hawker, C. J.; Bosman, A. W.; Harth, E. *Chem. Rev.* **2001**, *101*, 3661−3688.
(4) Chiefari, J.; Chong, Y. K.; Ercole, F.; Krstina, J.; Jeffery, J.; Le, T. P. T.; Mayadunne, R. T. A.; Meijs, G. F.; Moad, C. L.; Moad, G.; Rizzardo, E.; Thang, S. H. *Macromolecules* **1998**, *31*, 5559−5562.
(5) Brouwer, H. D.; Schellekens, M. A. J.; Klumperman, B.; Monteiro, M. J.; German, A. L. *J. Polym. Sci., Part A: Polym. Chem.* **2000**, *38*, 3596−3603.
(6) Otsu, T. *J. Polym. Sci., Part A: Polym. Chem.* **2000**, *38*, 2121−2136.
(7) Wayland, B. B.; Poszmik, G.; Mukerjee, S. L. *J. Am. Chem. Soc.* **1994**, *116*, 7943−7944.
(8) Destarac, M.; Bessiere, J. M.; Boutevin, B. *Book of Abstract, 213th ACS National Meeting* **1997**, POLY-315.
(9) Seymour, R. B.; Stahl, A. *J. Polym. Sci., Polym. Chem. Ed.* **1976**, *14*, 2545−2552.
(10) Stahl, G. A.; Seymour, R. B. *Polym. Sci. Technol.* **1977**, *10*, 217−230.
(11) Sato, T.; Iwaki, T.; Mori, S.; Otsu, T. *J. Polym. Sci., Polym. Chem. Ed.* **1983**, *21*, 819−828.
(12) Sato, T.; Iwaki, T.; Otsu, T. *J. Polym. Sci., Polym. Chem. Ed.* **1983**, *21*, 943−952.
(13) Sato, T.; Yutani, Y.; Otsu, T. *Polymer* **1983**, *24*, 1018−1022.
(14) Kafetzopoulos, C.; Valavanidis, A.; Yioti, I.; Hadjichristidis, N. *Polym. Int.* **1998**, *47*, 226−230.
(15) Zhang, H.; Hong, K.; Mays, J. W. *Macromolecules* **2002**, *35*, 5738−5741.
(16) Louis, P. E. J.; Gilbert, R. G.; Napper, D. H.; Teyssie, P.; Fayt, R. *Macromolecules* **1991**, *24*, 5746−5751.
(17) Reiss, H. *Science* **1987**, *238*, 1368−1373.
(18) El-Shall, M. S.; Bahta, A.; Rabeony, H.; Reiss, H. *J. Chem. Phys.* **1987**, *87*, 1329−1345.
(19) El-Shall, M. S.; Reiss, H. *J. Phys. Chem.* **1988**, *92*, 1021−1022.
(20) Murthy, S. K.; Olsen, B. D.; Gleason, K. K. *Langmuir* **2002**, *18*, 6424−6428.
(21) Meier, C. B.; Weickert, G.; van Swaaij, W. P. M. *J. Polym. Sci., Part A: Polym. Chem.* **2001**, *39*, 500−513.
(22) Behbahani, H. F.; Inoue, H. *J. Polym. Sci., Part B: Polym. Phys.* **1988**, *26*, 1519−1527.
(23) Chen, F. C.; Lackritz, H. S. *Macromolecules* **1997**, *30*, 5986−5996.
(24) Tsao, J. Y.; Ehrlich, D. *J. Appl. Phys. Lett.* **1983**, *42*, 997−999.
(25) Morita, H.; Sadakiyo, T. *J. Photochem. Photobiol. A: Chem.* **1995**, *87*, 163−167.
(26) Ulbricht, M.; Oechel, A.; Lehmann, C.; Tomaschewski, G.; Hicke, H.-G. *J. Appl. Polym. Sci.* **1995**, *55*, 1707−1723.
(27) Kubota, H.; Hata, Y. *J. Appl. Polym. Sci.* **1990**, *41*, 689−695.
(28) Allmer, K.; Hult, A.; Ranby, B. *J. Polym. Sci., Part A: Polym. Chem.* **1989**, *27*, 1641−1652.
(29) Ogiwara, Y.; Kanda, M.; Takumi, M.; Kubota, H. *J. Polym. Sci., Polym. Lett. Ed.* **1981**, *19*, 457−462.
(30) Bartlett, B.; Buckley, L. J.; Godbey, D. J.; Schroeder, M. J.; Fontenot, C.; Eisinger, S. *J. Vac. Sci. Technol.* **1999**, *B 17*, 90−94.

(31) Hsieh, M.-D.; Zellers, E. T. *Sens. Actuators* **2002**, *B 82*, 287−296.
(32) Wang, Y.; Chang, Y.-C. *Langmuir* **2002**, *18*, 9859−9866.
(33) Narita, H.; Kinoshita, H.; Araki, T. *J. Polym. Sci., Part A: Polym. Chem.* **1992**, *30*, 333−335.
(34) Piirma, I.; Chou, L.-P. *J. Appl. Polym. Sci.* **1979**, *24*, 2051−2070.
(35) Harwood, H. J.; Ritchey, W. M. *Polym. Lett.* **1965**, *3*, 419−426.
(36) Ito, K.; Yamashita, Y. *J. Polym. Sci.* **1965**, *B3*, 625−630.
(37) Kwon, T. S.; Kondo, S.; Kunisada, H.; Yuki, Y. *Polym. J.* **1998**, *30*, 559−565.
(38) Baek, K.-Y.; Kamigaito, M.; Sawamoto, M. *Macromolecules* **2001**, *34*, 215−221.
(39) Lyu, S.-P.; Cernohous, J. J.; Bates, F. S.; Macosko, C. W. *Macromolecules* **1999**, *32*, 106−110.
(40) Koulic, C.; Yin, Z.; Pagnoulle, C.; Gilbert, B.; Jerome, R. *Polymer* **2001**, *42*, 2947−2957.

MA021795S